ELSEVIER

Carbohydrate Research 279 (1995) 1–19

CARBOHYDRATE RESEARCH

Synthesis and conformational analysis of plant hormone (auxin) related compound 2-(indol-3-yl)ethyl β-D-galactopyranoside and its 2,3,4,6-tetra-*O*-acetyl derivative

Sanja Tomić [a], Biserka Kojić-Prodić [a,*], Volker Magnus [a], Goran Laćan [a], Helmut Duddeck [b], Monika Hiegemann [c]

[a] *Rudjer Bošković Institute, P.O.B. 1016, 10001 Zagreb, Croatia*

[b] *Universitaet Hannover, Institut fuer Organische Chemie, Schneiderberg 1B, D-30167 Hannover, Germany*

[c] *Ruhr-Universitaet Bochum, Lehrstuhl fuer Strukturchemie, Postfach 10 21 48, D-44780 Bochum, Germany*

Received 28 April 1995; accepted 26 June 1995

Abstract

The synthesis, structure analysis by X-ray diffraction and NMR spectroscopy (including $^1H\{^1H\}$NOEs) of 2-(indol-3-yl)ethyl 2,3,4,6-tetra-*O*-acetyl-β-D-galactopyranoside (**4**) are described. The per-*O*-acetylated derivative of 2-(indol-3-yl)ethyl β-D-galactopyranoside (**4***) was prepared along with the isomeric α-D-galactopyranose 1,2-orthoacetates (**3** *exo*- and *endo*-stereomers) by condensation of 2,3,4,6-tetra-*O*-acetyl-α-D-galactopyranosyl bromide (**1**) with the aglycone alcohol (**2**). The analogous condensation of **1** and 2-phenylethanol yielded a mixture of 2-phenylethyl 2,3,4,6-tetra-*O*-acetyl-β-D-galactopyranoside (**6**) and isomeric α-D-galactopyranose 1,2-orthoacetates (**5**). Compound **4** crystallized in the monoclinic system, space group $C2$, $a = 22.385(2)$, $b = 7.865(2)$, $c = 28.761(3)$ Å, $\beta = 102.1(1)°$, $Z = 8$, with two symmetrically independent molecules in the asymmetric unit. In both molecules β-D-galactopyranose rings are in the $^4C_1$ chair conformation. The conformational analysis of **4** and the analogous unprotected conjugate (**4***), based on molecular mechanics calculations and molecular dynamics simulations, is presented. The conformational stability about the bond of conjugation and relative orientation of the indole ring towards the β-D-galactopyranose moiety are discussed.

Keywords: Auxin; Galactopyranoside; X-ray diffraction; NMR spectroscopy; NOE; Molecular mechanics; Molecular dynamics

* Corresponding author.

SSDI 0008-6215(95)00245-6

1. Introduction

2-(Indol-3-yl)ethyl β-D-galactopyranoside (**4***) was detected as a conjugate of exogenously applied 2-(indol-3-yl)ethanol (**2**) in the unicellular algae *Euglena, Ochromonas* and *Chlorella* [1,2]. The aglycone alcohol **2** is generally present in plants [3,4] and is supposedly part of a regulatory mechanism affecting the level of the growth hormone (auxin), indole-3-acetic acid [5,6]. As judged by the biological activity of selected representatives, 2-(indol-3-yl)ethyl glycosides can be hydrolyzed and then reutilized for auxin biosynthesis [7,8]. They are also of interest as structural analogues of a compound of outstanding importance in plant hormone metabolism: 1-*O*-(indol-3-yl)acetyl-β-D-glucopyranose [9,10] which, because of its reactivity, cannot so far be converted to crystals suitable for X-ray diffraction analysis. This was, however, achieved for at least the per-*O*-acetyl derivatives of three 2-(indol-3-yl)ethyl glycosides, and computational methods then allowed us to predict the conformations of the deprotected glycosides. The biologically relevant conformational parameter, the relative orientation of the indole plane towards a side chain and its flexibility can be compared in these carbohydrate conjugates. We have already presented the results pertaining to the α-L-arabinopyranoside [11] and the β-D-xylopyranoside [12] and here we focus on β-D-galactopyranoside **4*** and its fully *O*-acetylated derivative **4**. The orientation of the sugar and the indole moieties, with respect to each other, is nearly the same and must thus be preferentially controlled by intramolecular forces. This is corroborated by computational methods, which predict only minor conformational changes when the acetyl groups are removed, and the resulting free glycosides transferred into aqueous solution. While the sugar moiety blocks the hydroxyl group of alcohol **2**, and thus prevents its oxidation into hormonally active indole-3-acetic acid, there is little steric interference with the indole nucleus. There are, therefore, important parallels to our previous results on the molecular structures of *N*-(indol-3-yl)acetyl amino acids [13–17] for which most indole ring-positions are also freely exposed. Accordingly, the conjugant moiety in *N*-(indol-3-yl)acetyl-L-aspartic and -L-glutamic acids does not protect the indole nucleus from enzymatic oxidation at the C-2 position [18–20], a reaction which is part of the catabolism of free indole-3-acetic acid as well [21]. In a similar fashion, the 2-(indol-3-yl)ethyl glycopyranosides studied may not be resistant to all catabolic enzymes attacking at the heterocyclic ring system, and they may also compete for certain hormone-binding sites of auxin "receptors".

2. Results and discussion

Synthesis.—Silver-oxide catalyzed condensation of 2,3,4,6-tetra-*O*-acetyl-α-D-galactopyranosyl bromide (**1**) and 2-(indol-3-yl)ethanol (**2**), in dichloromethane–diethyl ether solution, afforded the per-*O*-acetylated β-D-galactopyranoside **4** along with the isomeric α-D-galactopyranose 1,2-*O*-orthoacetates (**3**; *exo-* and *endo*-stereomers). The reaction times, the yields of products **3** + **4**, and the amounts of recovered halide **1**, summarized in Table 1, suggest that the rate of the condensation peaks at ether concentrations of 60–70%. The slow-down at lower ether levels was particulary dramatic and accompa-

Table 1
Condensation of galactopyranosyl bromide **1** with indole-3-ethanol (**2**) in dichloromethane–diethyl ether [a]

Ratio of CH_2Cl_2:Et_2O	Reaction time	**1** (%) recovered	Yield [b] (%) of **3** + **4**	Ratio of **3**:**4**	Ratio of **3** *exo*:**3** *endo*
100:0	6 days	46	28	38:62	11:89
90:10	6 days	42	25	39:61	15:85
75:25	6 days	43	22	37:63	20:80
70:30	6 days	29	40	36:64	12:88
65:35	6 days	7	61	24:76	18:82
60:40	6 days	1	78	25:75	23:77
60:40	16 h	73	18	22:78	31:69
55:45	16 h	23	63	18:82	25:75
50:50	16 h	n.d.	62	20:80	42:58
40:60	16 h	5	80	18:82	29:71
30:70	16 h	9	75	16:84	38:62
20:80	16 h	20	68	13:87	42:58
10:90	16 h	52	33	12:88	50:50
0:100	16 h	54	23	18:82	48:52

[a] Glycosyl halide **1** (1.1 mmol) and alcohol **2** (1.3 mmol) were reacted under identical conditions (see Experimental for details).
[b] Based on **1**.

nied by increased formation of orthoesters with the *endo*-isomer prevailing. Those solvent effects appear to be triggered by the indole moiety of alcohol **2**, as the condensation of halide **1** with 2-phenylethanol was complete within 16 h, regardless of the dichloromethane–diethyl ether ratio. Also, with the latter alcohol, the orthoesters always contained 60–70% of the *exo*-isomer and were most abundantly formed at ether concentrations of 20–40%, in essentially the same fashion as described for condensations of 2-phenylethanol and 2,3,4-tri-*O*-acetyl-β-L-arabinopyranosyl bromide [22]. Solvent effects in the corresponding reaction with indolic alcohol **2** have also been discussed [11].

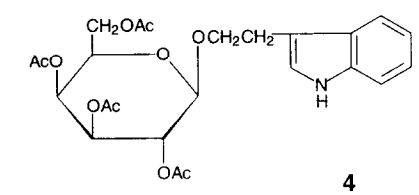

4

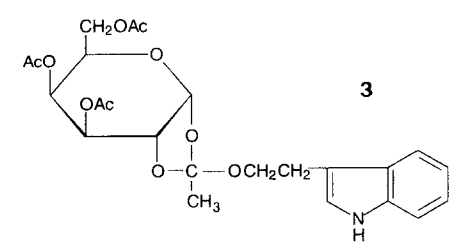

3

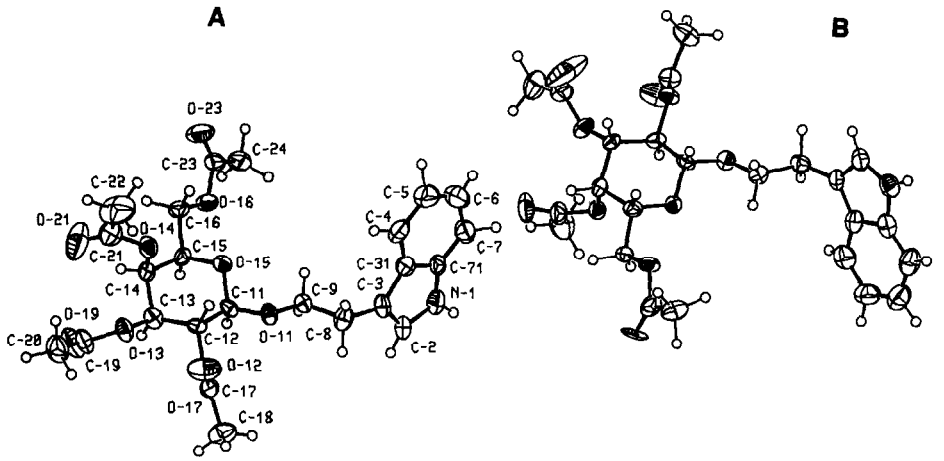

Fig. 1. The molecular structure (ORTEP drawing) of (indol-3-yl)ethyl 2,3,4,6-tetra-*O*-acetyl-β-D-galactopyranoside with atom numbering. The thermal ellipsoids are at the 30% probability level.

Deprotection of β-D-galactopyranoside **4** afforded the free glycoside **4***, which was identical to a major metabolite of alcohol **2** in certain unicellular algae [1,2].

X-ray structure analysis of **4**.—The structures of two symmetrically independent molecules of **4** with the atom numbering are shown in Fig. 1; the ORTEP [23] plot was drawn with thermal ellipsoids at the 30% probability level. Bond lengths and angles are listed in Tables 2 and 3, respectively. The endocyclic bonds C–O in the galactopyranose ring are symmetrical within the limits of experimental error: C-11–O-15, 1.429(9) Å (**A**), 1.424(12) Å (**B**); C-15–O-15, 1.422(9) Å (**A, B**). The equatorially disposed C-11–O-11 bonds, 1.387(9) Å (**A**), 1.389(9) Å (**B**) are significantly shorter than a normal C–O bond (1.428 Å), as is usually found for the anomeric C–O bond in equatorial glycopyranosides [24]. The values of the endocyclic angle C-11–O-15–C-15 are 111.1(6)° (**A**) and 111.7(7)° (**B**). These values are in agreement with the geometry of equatorial glycosidic bonds, typical of β-D-$^4C_1$ pyranosides [24]. The exocyclic valence angle at the glycosidic oxygen is enlarged to 115.9(6)° (**A**) and 114.7(5)° (**B**).

The geometry of the benzene part of indole nucleus deviates from that of a regular six-membered aromatic ring. Shortening of the C-5–C-6 bond [1.350(17) Å in the molecule **A**] and shrinkage of the C-6–C-7–C-71 angle [113.9(9)° (**A**), 118.1(9)° (**B**)] observed in **4** are in accord with the previous findings [11,12,14,15,25]. Drastic reduction of C-6–C-7–C-71 bond angle in the molecule **A** can be affected by somewhat higher thermal motion of the atom C-6 (U_{11} = 0.102 Å). However, low temperature data of *N*-(indol-3-yl)acetyl-L-norleucine [118.1(7)°] [16] and some ω-amino acid conjugates of IAA also revealed this trend [17].

The overall molecular conformation is described by the selected torsion angles presented in Table 4. The largest differences between the two symmetrically independent molecules are in the positions of the acetyl group attached to the O-13 atom, in molecule **A** the conformation about C-13–O-13 is (−) antiperiplanar whereas in **B** it is (−) anticlinal (Table 4).

Table 2
Bond lengths (Å) for 2-(indol-3-yl)ethyl 2,3,4,6-tetra-*O*-acetyl-β-D-galactopyanoside

	A	B
Pyranose moiety		
C-11–C-12	1.513(11)	1.500(11)
C-11–O-11	1.387(9)	1.389(9)
C-11–O-15	1.429(9)	1.424(12)
C-12–C-13	1.491(12)	1.513(12)
C-12–O-12	1.462(12)	1.468(12)
C-13–C-14	1.509(14)	1.529(13)
C-13–O-13	1.462(9)	1.432(9)
C-14–C-15	1.516(11)	1.515(11)
C-14–O-14	1.453(10)	1.451(10)
C-15–O-15	1.422(9)	1.422(9)
O-12–C-17	1.331(10)	1.358(9)
C-17–O-17	1.194(12)	1.206(12)
C-17–C-18	1.516(15)	1.466(15)
O-13–C-19	1.346(10)	1.319(14)
C-19–O-19	1.197(11)	1.144(19)
C-19–C-20	1.457(13)	1.469(16)
O-14–C-21	1.339(12)	1.345(10)
C-21–O-21	1.187(14)	1.205(10)
C-21–C-22	1.513(17)	1.488(13)
C-15–C-16	1.527(14)	1.497(13)
C-16–O-16	1.456(9)	1.450(10)
O-16–C-23	1.350(13)	1.351(13)
C-23–O-23	1.192(13)	1.188(13)
C-23–C-24	1.460(13)	1.488(13)
Tryptophol moiety		
N-1–C-2	1.404(12)	1.366(13)
N-1–C-71	1.368(14)	1.401(15)
C-2–C-3	1.359(13)	1.345(13)
C-3–C-31	1.456(14)	1.427(14)
C-31–C-71	1.383(12)	1.414(12)
C-31–C-4	1.401(16)	1.413(15)
C-4–C-5	1.399(17)	1.417(16)
C-5–C-6	1.350(17)	1.397(16)
C-6–C-7	1.385(18)	1.391(18)
C-7–C-71	1.401(15)	1.359(16)
C-3–C-8	1.493(12)	1.507(11)
C-8–C-9	1.489(12)	1.498(12)
C-9–O-11	1.421(10)	1.456(9)

The values of endocyclic torsion angles of the β-D-galactopyranose rings are found to be standard for β-D-$^4C_1$ saccharides [26]. The sugar rings conformations are described by the values of Cremer and Pople parameters [27]: $\theta = 5.6(3)°$; $\varphi = 24(3)°$; $Q = 0.586(3)$ Å (**A**); $\theta = 5.1(3)°$; $\varphi = 51(3)°$; $Q = 0.576(3)$ Å (**B**). The values of θ are the same

Table 3
Bond angles (°) for 2-(indol-3-yl)ethyl 2,3,4,6-tetra-*O*-acetyl-β-D-galactopyranoside

	A	B
Pyranose moiety		
C-11–O-15–C-15	111.1(6)	111.7(7)
O-15–C-11–C-12	108.5(7)	108.7(7)
C-11–C-12–C-13	109.3(6)	110.9(6)
C-12–C-13–C-14	111.9(8)	108.8(7)
C-13–C-14–C-15	109.0(7)	110.8(7)
O-15–C-15–C-14	110.5(6)	111.2(6)
C-9–O-11–C-11	115.9(6)	114.7(5)
O-11–C-11–C-12	108.2(6)	108.3(6)
O-15–C-11–O-11	108.2(7)	108.8(7)
O-12–C-12–C-11	105.6(7)	106.2(7)
O-12–C-12–C-13	109.2(7)	108.0(7)
O-13–C-13–C-12	105.9(6)	109.0(6)
O-13–C-13–C-14	108.7(7)	106.9(7)
O-14–C-14–C-13	109.7(6)	107.6(6)
O-14–C-14–C-15	107.9(7)	108.7(7)
O-15–C-15–C-16	108.0(7)	108.4(7)
C-14–C-15–C-16	111.8(7)	112.9(7)
C-15–C-16–O-16	104.5(7)	105.2(7)
Tryptophol moiety		
N-1–C-2–C-3	108.7(10)	117.0(10)
C-2–N-1–C-71	109.3(7)	108.9(8)
C-2–C-3–C-8	128.6(10)	129.4(9)
C-2–C-3–C-31	106.4(8)	105.2(7)
C-3–C-31–C-4	133.4(8)	132.9(8)
C-8–C-3–C-31	124.9(9)	125.4(8)
C-3–C-31–C-71	107.7(8)	109.5(8)
N-1–C-71–C-7	128.3(8)	131.0(9)
N-1–C-71–C-31	107.8(8)	104.6(9)
C-5–C-4–C-31	118.5(9)	117.8(8)
C-4–C-31–C-71	118.9(9)	117.8(9)
C-4–C-5–C-6	119.6(11)	121.8(11)
C-5–C-6–C-7	125.2(12)	120.2(11)
C-6–C-7–C-71	113.9(9)	118.1(9)
C-7–C-71–C-31	123.9(9)	124.3(10)
C-3–C-8–C-9	113.8(8)	112.0(7)
O-11–C-9–C-8	109.1(7)	106.9(6)

(within experimental error) in both molecules, **A** and **B**. Only the mode of distortion from the ideal *chair* form, described by φ, is different: in molecule **A** the distortion is towards *skew* and in molecule **B** towards *boat* conformation [26,28].

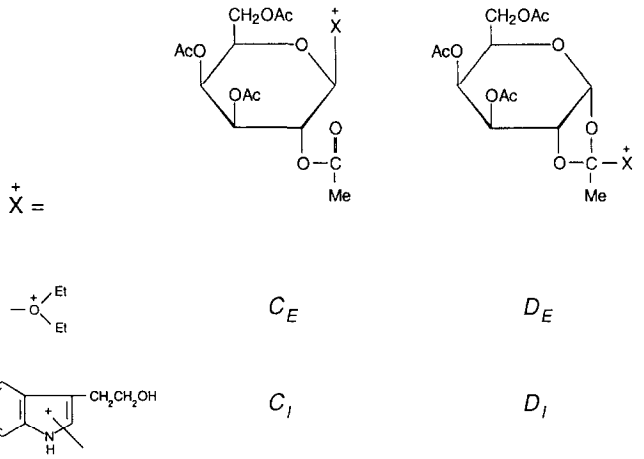

By the inspection of the Cambridge Structural Database [29], 26 compounds with the β-D-galactopyranose moiety were detected; among them there is the single example of a

Table 4
Selected torsion angles (°) for 2-(indol-3-yl)ethyl 2,3,4,6-tetra-*O*-acetyl-β-D-galactopyranoside

	A	B
Endocyclic angles		
O-15–C-11–C-12–C-13	59.4(9)	60.9(9)
C-11–C-12–C-13–C-14	−54.5(9)	−54.6(9)
C-12–C-13–C-14–C-15	52.0(8)	50.6(8)
C-13–C-14–C-15–O-15	−55.5(9)	−54.0(9)
C-14–C-15–O-15–C-11	63.8(8)	61.2(8)
C-15–O-15–C-11–C-12	−65.0(7)	−64.0(7)
Exocyclic angles		
C-15–O-15–C-11–O-11	177.9(5)	178.3(5)
O-15–C-11–C-12–O-12	177.0(5)	178.0(5)
C-11–C-12–C-13–O-13	−172.9(7)	−170.9(7)
C-12–C-13–C-14–O-14	−65.8(8)	−68.1(7)
D1 O-15–C-11–O-11–C-9	−68.3(9)	−69.1(9)
D2 C-11–O-11–C-9–C-8	−169.4(8)	−169.7(8)
Tryptophol moiety		
C-31–C-3–C-8–C-9	86(1)	85(1)
D3 O-11–C-9–C-8–C-3	−175.6(9)	−176.9(8)
D4 C-9–C-8–C-3–C-2	−91(1)	−94(1)
Angles between sugar ring and acetyl groups		
C-11–C-12–O-12–C-17	129.1(7)	137.6(7)
C-12–C-13–O-13–C-19	−155.5(9)	−113.9(9)
C-13–C-14–O-14–C-21	−103.3(9)	−95.6(9)
C-14–C-15–C-16–O-16	−164.3(6)	−160.8(6)

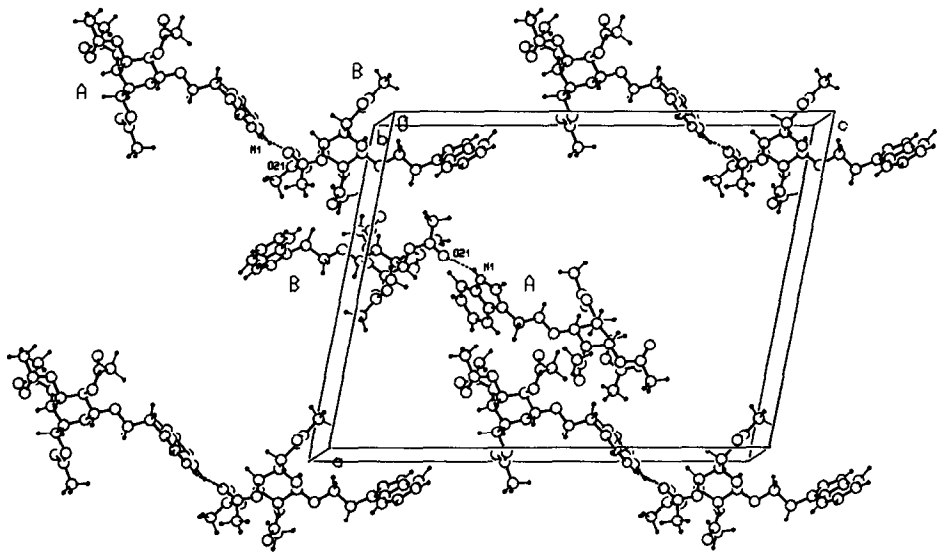

Fig. 2. The molecular packing of **4** with two independent molecules (**A** and **B**) in asymmetric unit.

chair $^1C_4$ conformation for methyl 2,3,4,6-tetra-*O*-acetyl-2-deoxy-2-fluoro-β-D-galactopyranoside [30].

The overall molecular shape of a Gal*p* conjugate of tryptophol was determined by the torsion angles about the C-3 → C-11 backbone. In both structures the aromatic plane is perpendicular to the side chain, D4 ≈ −90°; the conformations of the glycosidic torsion angle is (−) synclinal, and the conformation about the bond of conjugation O-11–C-9, as well as about the bond C-9–C-8, was (−) antiperiplanar (Table 4).

The crystal packing of β-D-Gal*p* conjugate is determined by N–H · · · O hydrogen bonds forming dimers between two crystallographically independent molecules of

Table 5
Hydrogen bond and C–H · · · O contacts in the crystal structures of 2-(indol-3-yl)ethyl 2,3,4,6-tetra-*O*-acetyl-β-D-galactopyranoside

	D · · · *A* (Å)	*D*–H (Å)	H · · · *A* (Å)	*D*–H · · · *A* (°)	Symmetry operations on *A*
(**A**)N-1–H [a] · · · O21(**B**)	2.885(8)	1.01(10)	2.17(10)	127(10)	$-x, y, -z$
(**A**)C-2–H · · · O23(**A**)	3.27(1)	0.97(9)	2.43(9)	144(9)	$-x, y-1, -z+1$
(**A**)C-9–H · · · O16(**A**)	3.52(1)	1.04(1)	2.53(9)	159(9)	$-x, y, -z+1$
(**A**)C-18–H · · · O11(**A**)	3.46(1)	1.08(1)	2.43(1)	159(1)	$1/2-x, 1/2+y-1, -z+1$
(**B**)C-2–H · · · O23(**B**)	3.35(1)	1.00(9)	2.55(9)	137(9)	$-x, y+1, -z$
(**B**)C-20–H [a] · · · O19(**A**)	3.38(1)	1.08(2)	2.37(1)	155(1)	$x, y+1, z-1$
(**B**)C-18–H [a] · · · O11(**B**)	3.43(1)	1.08(10)	2.44(1)	151(1)	$1/2-x, 1/2+y, -z$
(**B**)C-9–H · · · O16(**B**)	3.48(1)	1.01(9)	2.57(1)	149(9)	$-x, y, -z$

A and **B** are two crystallographically independent molecules. Atom numbering is given in Fig. 1.
[a] The H atom generated.

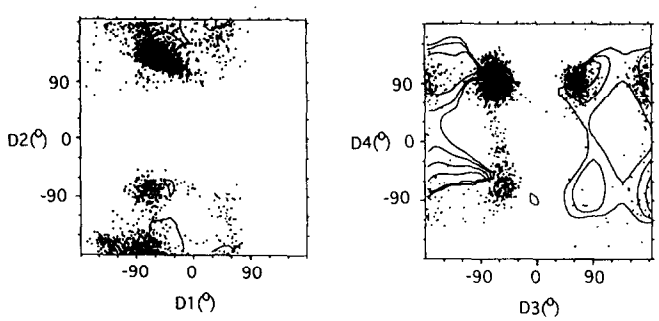

Fig. 3. The contour graphs for **4** obtained by rotation about pair of bonds: D1, D2 (with D3 −sc, D4 ≈ −90°) and D3, D4, (with D1 −sc, D2 ac) (CVFF). The values obtained during 710 ps of MD simulations in vacuo at room temperature are superimposed. [D1(O-15–C-11–O-11–C-9), D2 (C-11–O-11–C-9–C-8), D3 (O-11–C-9–C-8–C-3), D4 (C-2–C-3–C-8–C-9)]. The contour lines are drawn at an interval of 2 kcal/mol.

β-D-Gal*p* conjugate (Fig. 2) and the number of C–H · · · O interactions (Table 5). Recently, more information on this type of contact and its function has appeared in the literature [31–34]. The neutron diffraction data of the crystal structure of vitamin B_{12} coenzyme at 15 K offer more accurate data on the C–H · · · O contacts [31].

Molecular mechanics and molecular dynamics in vacuo for **4** *and* **4***.—Optimization of the crystallographically determined structure of **4**, performed for each molecule (**A**, **B**) separately, as well as for molecules treated as an adduct (**A** + **B**) was performed to see if the conformation of **4** determined in crystal is global minimum. During the optimization the antiperiplanar orientation about the bond C-9–O-11 (D2), as it appears in the crystal, changed to anticlinal. The comparative conformational analysis (MM + MD) on **4** and **4*** was carried out in order to see the influence of *O*-peracetylation on the relative orientation of the indole plane towards the sugar moiety. The results obtained on **4** and **4*** are similar and can be summarized as follows: D1 is mostly (−) synclinal, D2 is either anticlinal or antiperiplanar, while for D3 all three staggered conformations are possible (± synclinal and antiperiplanar), D4 is about ±90° (Figs. 3

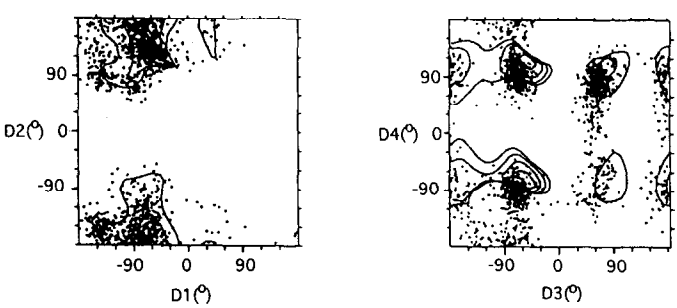

Fig. 4. The contour graphs for **4*** obtained by rotation about pair of bonds: D1, D2 (with D3 −sc, D4 ≈ −90°) and D3, D4, (with D1 −sc, D2 ac) (CVFF). The values obtained during 250 ps of MD simulations in vacuo at temperature increasing from 300 → 400 K are superimposed. The contour lines are drawn at an interval of 2 kcal/mol.

Table 6
Relative energies of the representative conformers of **4** and **4*** energy minimized in three different force fields: (a) CVFF, (b) AMBER-Homans modified and (c) cff91. The conformers are selected from the most populated regions obtained during MD simulations in vacuo. During the optimizations (DISCOVER) a constant force of 20 kcal/mol has been used to preserve conformations of torsions D1 → D4

Torsion angles (°) (D1, D2, D3, D4)	ΔE_{konf} (kcal/mol)			
	4	**4***		
	(a)	(a)	(b)	(c)
G1* (−sc, ap, ap, −ac)	6	5	1	5
G2* (−sc, ap, sc, ac)	3	5	0	6
G3* (−sc, ap, sc, −ac)	5	6	2	6
G4* (sc, ap, −sc, ac)	6	9	1	8
G5* (−sc, ap, −sc, −ac)	5	5	0	5
G6* (−sc, ac, ap, ac)	6	8	3	8
G7* (−sc, ac, −sc, −ac)	0	0	2	0
G8* (−sc, ac, −sc, ac)	1	1	3	1
G9* (−sc, ac, sc, ac)	7	6	2	6
G10* (−sc, ac, sc, −ac)	8	7	2	13
G11* (−sc, ap, ap, ac)	6	5	1	5

Legend: synclinal (sc), anticlinal (ac), antiperiplanar (ap) [35].

and 4). To determine relative energy between the most frequent conformers detected during MD simulations, energy minimizations were performed with tethering atoms connecting indole and sugar rings to starting conformation. The results are given in Table 6 [35]. The lowest conformational energies are determined for the conformations G7 and G7* with D1 (−) synclinal, D2 anticlinal, D3 (−) synclinal and D4 (−) anticlinal, with CVFF [36] and cff91 [37] force fields and for the conformers G2* (D1 = −sc, D2 = ap, D3 = sc, D4 about 90°, Table 6) and G5* (D1 = −sc, D2 = ap, D3 = −sc, D4 about −90°, Table 6), with AMBER-Homans modified force field [38].

Conformations of **4*** *and* **4** *in solution.*—To simulate natural conditions and to evaluate the influence of solvent on the conformational behaviour of the compound, a molecular dynamics study was performed in periodic boxes of water.

The conformer with the relative orientation of the rings (sugar and indole) as determined by X-ray diffraction analysis (G1*) did not remain stable during the simulations in water at room temperature. During the simulations with AMBER-Homans modified force field transitions of D3 from ap to ac conformation occurred about 30 ps from the beginning followed by the transition of D4 from ≈ −90° to ≈ 90°; i.e., transformation of conformer G1* to G2* (see Table 6) occurred. G2* remained stable during about 150 ps of the simulation (Fig. 5). At the end of the simulations the molecule returned to G1*. Similar transitions occurred during the simulations with CVFF. The conformation G7*, determined as global minimum in CVFF and cff91, remained stable during about 80 ps of simulation at increasing temperature (CVFF) (50 ps at 300 K + 30 ps at 330 K, Fig. 6), at higher temperatures (350 → 450 K) transitions of D3 from −sc → ap → sc occurred and fluctuations of D1 (from −60° to 180°), D2 (from about ±120° to 180°) and D4 (from −90° to 90°) became frequent. The results of

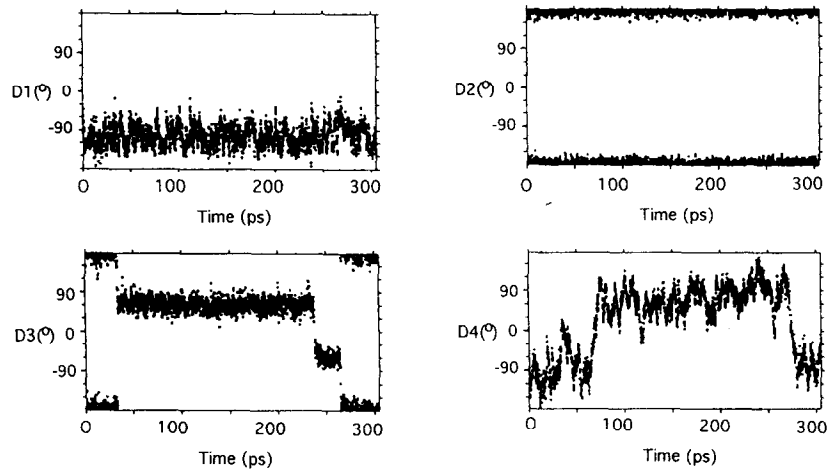

Fig. 5. The MD simulations for **4*** (conformation G1* from Table 6), in water (AMBER-Homans modified force field); variations of torsion angles D1, D2, D3 and D4 (in degrees) are given. Conditions of the simulation are described in the text.

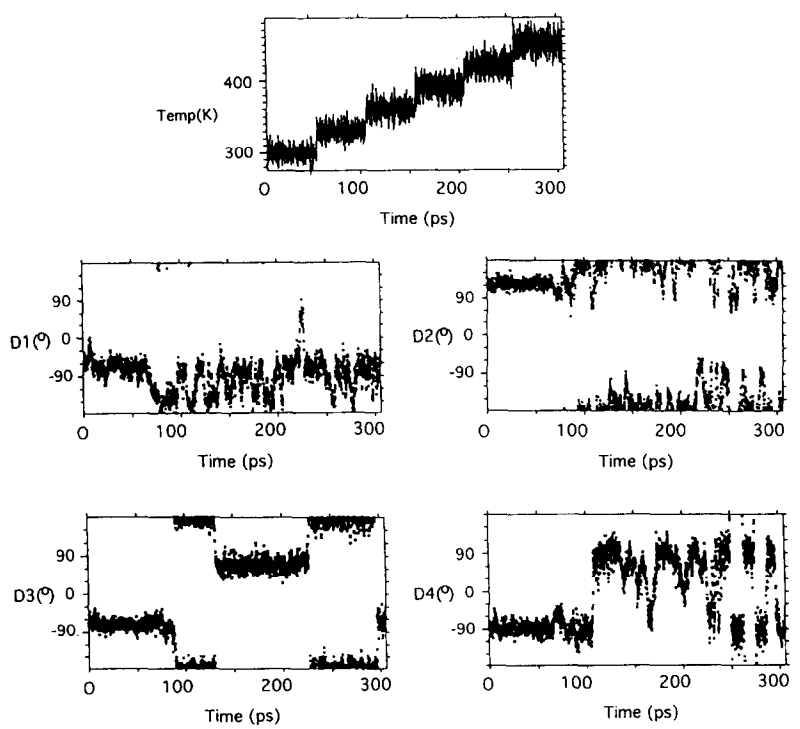

Fig. 6. The MD simulations for **4*** (conformation G7* from Table 6), in water (CVFF); variations of temperature and torsion angles D1, D2, D3 and D4 are given. Conditions of the simulation are described in the text.

the simulations at room temperature can be summarized as follows: D2 was mostly antiperiplanar or anticlinal; D1 oscillated between (−) synclinal and (−) anticlinal; for D3 all three staggered conformations occurred with approximately equivalent frequency; and D4 oscillated between (−) and (+) 90°. By NOE-difference and ROSY signals steric contacts have been determined (compound **4**) for H-8 and H-2, H-8 and H-4, H-8 and both H-9/H-9′, H-8 and H-11, both H-9/H-9′ and H-4 as well as H-2. As the comparative analysis of the results (variations on D1 → D4) obtained for **4*** and **4** has not revealed any significant difference (i.e., similarity of the orientation of the indole plane towards the sugar moiety of a free conjugate and its peracetylated derivative has been maintained in water medium) variations of some H · · · H distances (relevant for the overall conformation of the molecule) determined during MD simulations (of **4*** and **4**) were compared with the results of NOE analysis (on **4**). During the simulations in water distances between both H-8/H-8′ and H-4 and H-2 were mostly below 4 Å (in the range of 2.5–4.4 Å); medium intensity of NOE-signals measured. Distances between both H-9/H-9′ and H-4 and H-2, and both H-8/H-8′ and H-11 were about 4.5 Å (in the range 2.5–5 Å); low intensity of NOE-signals measured. Findings of MD simulations in water are in accord with measured NOEs which should be treated as averaged signals produced from all conformers with the reasonable populations. NOE-difference and NOESY signals were observed within the indole and galactose moieties as expected.

A conformational search performed by rotations about pair of bonds (D1 → D4) for **4** and **4***, and molecular dynamics simulations in vacuo and water revealed the most stable conformations of molecules analyzed and the most frequent transitions between the minima. In all force fields used the conformation of **4***, equivalent to the conformation of **4** determined in crystal, is one of quite a few local minima determined (see Table 6). These conformers appeared to be relatively stable during MD simulations in water; transitions among them occurred within hundreds of ps at room temperature.

3. Experimental

General.—Melting points were determined in open capillaries and are reported uncorrected. Optical rotations were measured with a Zeiss Kreispolarimeter. Routine ^{1}H-NMR spectra were recorded at 90 MHz, with a digital resolution of 0.2 Hz, using Me_4Si as an internal standard. However, for **4** spectra were recorded at 400.1 MHz, and practically all signals are first-order (except H-16/H-16′). Analytical TLC was performed on Silica Gel GF (Merck) with detection by UV fluorescence and by spraying with 10% H_2SO_4 in EtOH and heating. Preparative chromatography was accomplished by TLC on Silica Gel PF_{254} (Merck) or on a column (65 × 2 cm) containing a mixture of Silica Gel H (65 g) and Celite (40 g) (Kemika, Zagreb, Croatia). The eluents were: A (20:3 CH_2Cl_2–diethyl ether) and B (8:2 CH_2Cl_2–MeOH). 2,3,4,6-Tetra-*O*-acetyl-α-D-galactopyranosyl bromide (**1**) [39] was prepared by treating a dichloromethane solution of β-D-galactopyranose tetraacetate [40] with 32% hydrogen bromide in glacial acetic acid [41].

*Condensation of 2,3,4,6-tetra-*O*-acetyl-α-*D*-galactopyranosyl bromide* (**1**) *with 2-(indol-3-yl)ethanol* (**2**).—Reactions were performed in the dark, at room temperature,

using the solvents and reaction times specified in Table 1. To a vigorously stirred suspension of alcohol **2** (209 mg, 1.3 mmol), solvent (20 mL), freshly prepared, dry Ag_2O (0.15 g, 0.65 mmol) and anhydrous $CaSO_4$ (0.5 g) was added, in small portions through 1 h, a solution of **1** (stabilized with 5% $CaCO_3$; 452 mg, 1.1 mmol) in the same volume of solvent. The mixture was further stirred for the time required. Insoluble material was removed by centrifugation; the supernatant was concentrated and immediately passed through a column of silica gel–Celite eluted with solvent A to yield, in this order: *(a)* unreacted halide **1**, *(b)* a mixture of the *exo*- and *endo*-isomers of orthoester **3**, and *(c)* the per-*O*-acetylated β-D-galactopyranoside **4**. TLC (solvent A) of the crude reaction mixture also showed residual alcohol **2** and a sugar derivative with chromatographic properties as expected for 2,3,4,6-tetra-*O*-acetyl-D-galactopyranose; these two compounds were not isolated. The material eluted from the column was processed as follows:

(a) 2,3,4,6-Tetra-*O*-acetyl-α-D-galactopyranosyl bromide (**1**). The compound was identified by its ^{1}H-NMR spectrum.

(b) 3,4,6-Tri-*O*-acetyl-1,2-*O*-{1-[2-(indol-3-yl)ethoxy]ethylidene}-α-D-galactopyranose (**3**). Preparative TLC (multiple development with 20:1 CH_2Cl_2–diethyl ether) afforded, after drying in vacuo at 60 °C, the title compound as an amorphous white solid. ^{1}H-NMR data (CD_3Cl), *exo*-isomer: δ 5.66 (d, 1 H, $J_{1,2}$ 4.8 Hz, H-1), 5.04 (dd, 1 H, $J_{2,3}$ 6.5,$J_{3,4}$ 3.4 Hz, H-3), 5.40 (dd, 1 H, $J_{4,5}$ 2.3 Hz, H-4), 4.06–4.30 (m, 4 H, H-2, H-5, H-6, H-6′), 2.08 (s, 3 H, OAc), 2.03 (s, 6 H, 2 OAc), 1.68 (s, 3 H, ethylidene CH_3), 3.02 (t, 2 H, *J* 7.3 Hz, $ArCH_2$), 3.79 (t, 2 H, $ArCH_2CH_2O$), 8.07 (broad s, 1 H, indole NH), 7.02–7.66 (m, 5 H, indole CH); *endo*-isomer: δ 1.61 (s, 3 H, ethylidene CH_3); other signals not sufficiently distinct in mixtures with the *exo*-stereomer. Anal. Calcd for $C_{24}H_{29}NO_{10}$ (491.49): C, 58.63; H, 5.95; N, 2.85. Found: C, 58.73; H, 6.04; N, 2.70.

(c) 2-(Indol-3-yl)ethyl 2,3,4,6-tetra-*O*-acetyl-β-D-galactopyranoside (**4**). Recrystallization from CH_2Cl_2–hexane gave white crystals; mp 156–158 °C; $[\alpha]_D$ −15.5° (*c* 1, $CHCl_3$); ^{1}H-NMR data ($CDCl_3$): δ 4.47 (d, 1 H, $J_{11,12}$ 8.0 Hz, H-11), 5.22 (dd, 1 H, $J_{12,13}$ 10.6 Hz, H-12), 4.97 (dd, 1 H, $J_{13,14}$ 3.4 Hz, H-13), 5.37 (dd, 1 H, $J_{14,15}$ 1.2 Hz, H-14), 3.86 (dt, 1 H, $J_{15,16} = J_{15,16'} = 6.8$ Hz, H-15), 4.15 (dd, 1 H, $J_{16,16'}$ 11.2 Hz, H-16), 4.12 (dd, 1 H, H-16′), 2.12, 2.01, 1.96, 1.83 (4 s, 4 × 3 H, CH_3-18, CH_3-20, CH_3-22, CH_3-24), 8.11 (broad s, 1 H, NH), 7.02(d, 1 H, $J_{2,8}$ 2.4 Hz, H-2), 7.56 (dm, 1 H, $J_{4,5}$ 8.0 Hz, H-4), 7.09 (ddd, 1 H, $J_{5,6}$ 7.2, $J_{5,7}$ 1.2 Hz, H-5), 7.18 (dd, 1 H, $J_{6,7}$ 8.2 Hz, H-6), 7.33 (ddd, 1 H, $J_{4,7}$ 1.0 Hz, H-7), 3.04 (tm, 2 H, $J_{8,9} = J_{8,9'} = 7.0$ Hz, H-8), 4.17 (overlapped by H-16, 1 H, H-9, pro-*S*), 3.76 (dt, 1 H, $J_{9,9'}$ 9.6 Hz, H-9′, pro-*R*). Anal. Calcd for $C_{24}H_{29}NO_{10}$ (491.49): C, 58.63; H, 5.95; N, 2.85. Found: C, 58.92; H, 6.03; N, 2.82.

Condensation of halide **1** *with 2-phenylethanol.*—2-Phenylethanol, reacted as described above for alcohol **2**, afforded a mixture of *(a)* 3,4,6-tri-*O*-acetyl-1,2-*O*-[1-(2-phenylethoxy)ethylidene]-α-D-galactopyranose (**5**) and *(b)* 2-phenylethyl 2,3,4,6-tetra-*O*-acetyl-β-D-galactopyranoside (**6**). Halide **1** was always completely consumed within 16 h. The results of eight experiments summarized as groups of numbers in parentheses (i.e., per cent of diethyl ether in the solvent, per cent yield of **5** + **6** based on halide **1**, per cent of **5** in mixture of **5** + **6**, per cent *exo*-isomer in **5**) were: (0, 64, 0.2, not

determined); (10, 46, 8, 62); (20, 65, 50, 70); (30, 57, 42, 60); (40, 61, 44, 65); (60, 57, 25, 58); (80, 53, 3, 60); (100, 59, 0, —). The second solvent component was CH_2Cl_2. Further characterization was as follows:

(a) 3,4,6-Tri-*O*-acetyl-1,2-*O*-[1-(2-phenylethoxy)ethylidene]-α-D-galactopyranose (**5**). Preparative TLC (solvent A) gave the title compound (mixture of *exo*- and *endo*-isomers) as an amorphous solid. ^{1}H-NMR data ($CDCl_3$), *exo*-isomer: δ 5.61 (d, 1 H, $J_{1,2}$ 4.8 Hz, H-1), 5.06 (dd, 1 H, $J_{2,3}$ 6.8, $J_{3,4}$ 3.4 Hz, H-3), 5.40 (dd, 1 H, $J_{4,5}$ 2.3 Hz, H-4), ca. 4.1 (m, 4 H, H-2, H-5, H-6, H-6′), 2.09 (s, 3 H, OAc), 2.06 (s, 6 H, 2 OAc), 1.65 (s, 3 H, ethylidene CH_3), 7.25 (m, 5 H, phenyl ring), 2.86 (t, 2 H, *J* 7.2 Hz, $ArCH_2$), 3.72 (t, 2 H, $ArCH_2CH_2O$); *endo*-isomer: only selected signals were discernible in mixtures with the *exo*-isomer, i.e., δ 5.66 (d, 1 H, $J_{1,2}$ 4.4 Hz, H-1), 2.09, 2.07, 2.06 (3 s, 3 × 3 H, 3 OAc), 1.58 (s, 3 H, ethylidene CH_3), 2.91 (t, 2 H, *J* 6.8 Hz, $ArCH_2$). Anal. Calcd for $C_{22}H_{28}O_{10}$ (452.46): C, 58.40; H, 6.24. Found: C, 58.27; H, 6.14.

(b) 2-Phenylethyl 2,3,4,6-tetra-*O*-acetyl-β-D-galactopyranoside (**6**). Preparative TLC (solvent A) afforded the title compound as an amorphous solid. ^{1}H-NMR data ($CDCl_3$): δ 4.45 (d, 1 H, $J_{1,2}$ 7.5 Hz, H-1), 5.22 (dd, 1 H, $J_{2,3}$ 10.4 Hz, H-2), 4.97 (dd, 1 H, $J_{3,4}$ 3.3 Hz, H-3), 5.38 (dd, 1 H, $J_{4,5}$ 0.9 Hz, H-4), 3.9–4.2 (m, 4 H, H-5, H-6, H-6′, $ArCH_2CH_aH_bO$), 2.15, 2.05, 1.97, 1.89 (4 s, 4 × 3 H, 4 OAc), 2.90 (t, 2 H, averaged J_{vic} 6.8 Hz, $ArCH_2$), 3.67 (dt, 1 H, J_{vic} 7.3, J_{gem} 9.4 Hz, $ArCH_2CH_aH_bO$). Anal. Calcd for $C_{22}H_{28}O_{10}$ (452.46): C, 58.40; H, 6.24. Found: C, 58.49; H, 6.46.

2-(Indol-3-yl)ethyl β-D-galactopyranoside (**4***).—Sodium methylate (2 mg) was added to a solution of per-*O*-acetylated β-D-galactopyranoside **4** (220 mg) in methanol (10 mL) and the mixture was kept at room temperature until TLC (solvent B) indicated complete deacetylation (1.5 h). Following neutralization with Dowex 50X8 the solution was concentrated and subjected to preparative TLC (7:1 CH_2Cl_2–MeOH). The main product ($R_f = 0.5$) was eluted with acetone to yield, on evaporation of the solvent, the monohydrate of the title compound as an amorphous, hygroscopic white solid (134 mg, 93%); $[\alpha]_D$ −20° (*c* 0.75, 95% EtOH). Anal. Calcd for $C_{16}H_{21}NO_6 \cdot H_2O$ (341.36) C, 56.50; H, 6.75; N, 4.11. Found: C, 56.66; H, 6.54; N, 3.91.

$^1H\{^1H\}$NOE measurements.—The steady state NOE-difference spectra were measured for **4** in $CDCl_3$ at 400.1 MHz (Bruker AM-400) using a standard pulse technique. Details have been described by us before [13]. Longitudinal relaxation times were estimated not to exceed 2 s.

ROSEY spectrum (standard pulse sequence): spin-lock time in different experiments 80, 120, 160, 250, 300 and 400 ms (optimal results with 300 ms), relaxation delay 3.5 s, data matrix 2K × 2K (512 experiments with 2K zero filling in F1, 2K data print in F2); digital resolution 3.3 Hz/point in F2 with a spectral width of 2127 Hz and 32 transients in each experiment.

X-ray structure determination of **4**.—Crystals suitable for X-ray analysis were grown from 1:1 (v/v) MeOH-*iso*PrOH at room temperature in the dark, during a few days. Compound **4** crystallized in the space group *C*2 with two molecules per asymmetric unit. The crystal data and a summary of the experimental details are listed in Table 7. X-ray intensity data were collected on an Enraf–Nonius CAD4 diffractometer with Mo$K\alpha$ radiation. There were no significant variations in intensity for standard reflec-

Table 7
Crystal data and symmary of experimental details of **4**

Molecular formula	$C_{24}H_{29}NO_{10}$
M_r	491.49
Crystal size (mm)	$0.5\times0.5\times0.3$
a (Å)	22.385(2)
b (Å)	7.865(2)
c (Å)	28.761(3)
β (°)	102.1(1)
V (Å^3)	4951.2(2)
Crystal system	monoclinic
Space group	$C2$
D_x (g cm^{-3})	1.319
Z	8
μ(Mo$K\alpha$) (cm^{-1})	0.97
F (000)	2080
T (K)	296(2)
No. of reflections used for cell parameters	25
θ range (°) used for cell parameters	7.0–17.0
θ range for intensity measurement (°)	2.0–25.0
hkl range	$(-1, 21; -1, 7; -27, 27)$
$\omega/2\theta$ scan	$0.80+0.35\tan\theta$
No. of measured reflections	5488
No. of symm. independent refl. with $I>2\sigma(I)$	4650
No. of variables	741
R	0.062
R_w ($w=1.7225/[\sigma^2(F_o)+0.001379F_o^2]$)	0.064
S	2.6
Final shift/error	<0.5
Residual electron density$(\Delta\rho)_{max}$, $(\Delta\rho)_{min}$ (e Å^{-3})	0.33, −0.35

tions. The data were corrected for Lorentz and polarization effects. According to the calculated density, there were eight molecules per unit cell. The structure was solved by the SHELX86 [42] programme. Refinement was by full-matrix least-squares on F minimizing $\Sigma w(|F_o|-|F_c|)^2$ with the SHELX77 programme [43]. The H atom coordinates were determined from the subsequent difference Fourier syntheses, whereas the H atoms attached to the acetyl groups (C-18, C-20, C-22, C-24) and to the benzene part of the indole ring were calculated on the stereochemical grounds. Those calculated on the theoretical grounds were refined riding on their respective C atoms. Atomic scattering factors were those included in SHELX77. Details of the refinement procedure are given in Table 7. In the structure determination of **4**, the D-enantiomer was selected according to the assignment (*R*) at the C-15 atom. Final atomic coordinates and equivalent isotropic thermal parameters are given in Table 8 [1]. The molecular geometry was

[1] Tables of atomic coordinates, bond lengths, and bond angles have been deposited with the Cambridge Crystallographic Data Centre. These tables may be obtained, on request, from the Director, Cambridge Crystallographic Data Centre, 12 Union Road, Cambridge, CB2 1EZ, UK.

Table 8
Final atomic coordinates and equivalent isotropic thermal parameters for 2-(indol-3-yl)ethyl 2,3,4,6-tetra-*O*-acetyl-β-D-galactopyranoside

Atom	Molecule A				Molecule B			
	x	*y*	*z*	U_{eq} [a] (Å^2)	*x*	*y*	*z*	U_{eq} [a] (Å^2)
O-11	0.1295(2)	0.281(1)	0.4912(2)	0.036(2)	0.1348(2)	0.5843(10)	0.0141(2)	0.036(2)
O-12	0.1778(2)	0.0457(9)	0.5605(2)	0.037(2)	0.1463(2)	0.8242(9)	−0.0534(2)	0.037(2)
O-13	0.2193(2)	0.200(1)	0.6526(2)	0.045(2)	0.1358(2)	0.6767(10)	−0.1484(2)	0.047(2)
O-14	0.1950(2)	0.536(1)	0.6310(2)	0.043(2)	0.1277(2)	0.3499(10)	−0.1284(2)	0.034(2)
O-15	0.1067(2)	0.463(1)	0.5468(2)	0.035(2)	0.0832(2)	0.4037(9)	−0.0428(2)	0.034(2)
O-16	0.0141(2)	0.684(1)	0.5675(2)	0.043(2)	−0.0201(2)	0.1802(10)	−0.0669(2)	0.039(2)
O-17	0.2769(3)	0.077(1)	0.5611(3)	0.070(3)	0.2412(3)	0.8024(12)	−0.0671(3)	0.075(3)
O-19	0.1703(3)	0.122(1)	0.7089(2)	0.082(3)	0.0893(6)	0.9112(16)	−0.1711(4)	0.164(6)
O-21	0.2161(4)	0.545(2)	0.7106(3)	0.111(4)	0.1049(3)	0.3459(13)	−0.2088(2)	0.068(2)
O-23	0.0203(3)	0.964(1)	0.5789(2)	0.067(3)	−0.0191(3)	−0.1005(11)	−0.0793(3)	0.048(3)
N-1	−0.0311(3)	0.334(1)	0.3039(2)	0.049(3)	0.0705(3)	0.5439(13)	0.2006(3)	0.047(3)
C-2	0.0033(4)	0.232(1)	0.3399(3)	0.044(3)	0.0879(4)	0.6353(15)	0.1653(3)	0.049(3)
C-3	0.0507(3)	0.325(1)	0.3641(3)	0.040(3)	0.1204(3)	0.5403(13)	0.1406(2)	0.037(3)
C-4	0.0818(5)	0.639(2)	0.3499(3)	0.059(4)	0.1534(4)	0.2237(15)	0.1534(3)	0.054(3)
C-5	0.0634(5)	0.782(2)	0.3212(4)	0.069(4)	0.1476(5)	0.0810(15)	0.1822(4)	0.064(4)
C-6	0.0122(6)	0.774(2)	0.2868(4)	0.074(5)	0.1142(5)	0.0886(18)	0.2181(4)	0.066(4)

C-7	−0.0242(5)	0.631(1)	0.2756(3)	0.059(4)	0.0868(4)	0.2402(17)	0.2273(3)	0.059(4)
C-8	0.0977(3)	0.275(1)	0.4072(3)	0.047(3)	0.1462(4)	0.5876(14)	0.0980(3)	0.044(3)
C-9	0.0803(4)	0.322(1)	0.4529(3)	0.038(3)	0.1037(3)	0.5417(14)	0.0522(3)	0.038(3)
C-11	0.1167(3)	0.289(1)	0.5363(3)	0.030(3)	0.0982(3)	0.5768(12)	−0.0313(3)	0.034(2)
C-12	0.1722(3)	0.226(1)	0.5716(3)	0.034(2)	0.1341(3)	0.6446(12)	−0.0658(3)	0.032(2)
C-13	0.1614(3)	0.243(1)	0.6207(3)	0.039(3)	0.0970(3)	0.6368(12)	−0.1162(3)	0.032(3)
C-14	0.1438(3)	0.422(1)	0.6311(3)	0.034(3)	0.0747(3)	0.4544(12)	−0.1270(3)	0.030(3)
C-15	0.0912(3)	0.479(1)	0.5921(3)	0.033(3)	0.0442(3)	0.3874(12)	−0.0884(3)	0.034(3)
C-16	0.0742(3)	0.665(1)	0.5985(3)	0.041(3)	0.0253(4)	0.2051(12)	−0.0956(3)	0.034(3)
C-17	0.2320(4)	−0.009(1)	0.5546(3)	0.039(3)	0.2030(3)	0.8858(14)	−0.0534(3)	0.042(3)
C-18	0.2277(4)	−0.192(2)	0.5368(3)	0.061(3)	0.2089(4)	1.0632(14)	−0.0374(3)	0.059(3)
C-19	0.2175(4)	0.144(2)	0.6965(3)	0.055(3)	0.1269(6)	0.8163(16)	−0.1744(3)	0.064(4)
C-20	0.2780(4)	0.119(2)	0.7262(3)	0.069(4)	0.1711(5)	0.8272(19)	−0.2055(3)	0.086(5)
C-21	0.2269(5)	0.586(2)	0.6736(4)	0.065(4)	0.1402(4)	0.3217(14)	−0.1715(3)	0.045(3)
C-22	0.2803(5)	0.695(2)	0.6672(5)	0.108(5)	0.2047(4)	0.2664(18)	−0.1671(3)	0.077(4)
C-23	−0.0081(4)	0.844(1)	0.5615(3)	0.044(3)	−0.0386(4)	0.0189(14)	−0.0620(3)	0.050(3)
C-24	−0.0706(4)	0.839(1)	0.5334(3)	0.053(3)	−0.0889(4)	0.0214(15)	−0.0354(3)	0.060(3)
C-31	0.0468(4)	0.491(1)	0.3412(3)	0.042(3)	0.1253(3)	0.3772(13)	0.1628(3)	0.040(3)
C-71	−0.0044(3)	0.490(1)	0.3047(3)	0.038(3)	0.0928(4)	0.3776(15)	0.2000(3)	0.046(3)

[a] $U_{eq} = \frac{1}{3}\Sigma_i\Sigma_j\ U_{ij}\ a_i^* \cdot a_j^*\ \boldsymbol{a}_i \cdot \boldsymbol{a}_j$.

calculated by the programme EUCLID [44]. Drawings were prepared by the programme PLUTON incorporated in EUCLID and ORTEPII [23]. Calculations were performed on the computers Micro-VAX II and Silicon Graphics INDIGO2, at the X-ray Laboratory of the Rudjer Bošković Institute, Zagreb, Croatia.

Molecular mechanics and molecular dynamics for **4** *and* **4***.—Molecular mechanics and dynamics calculations were carried out on 2-(indol-3-yl)ethyl β-D-galactopyranoside (**4***) and its *O*-peracetylated derivative (**4**) using the programme DISCOVER [45], version 2.96 [45], with the CVFF [36], AMBER-Homans modified [38] and cff91 [37] force fields. According to our previous MM and MD results on sugar and other IAA derivatives [11,12,15,25] CVFF (as well as cff91) is suitable for the analysis of **4*** and **4**, AMBER-Homans modified force field was used by the other authors for the analysis of polysaccharides and glycoconjugates [38,46,47].

Tethering of selected atoms to desired conformation was utilized using penalty function with the harmonic force constant of 20 kcal/(mol Å^2) [36,48]. Molecular mechanics calculations were accompanied with molecular dynamics simulations in vacuo in order to explore conformational space of compounds **4** and **4*** in more detail, especially possible conformational transitions. The rotations about two pairs of the relevant bonds (C-11 → C-3), in steps of 9° (CVFF), performed for the compounds **4** and **4*** were followed by 720 ps of molecular dynamics simulations in vacuo at 300 K for **4** (Fig. 3) and over a range of temperatures (300 → 400 K) for **4***, 250 ps (Fig. 4). In water, simulations were carried out using periodic boundary conditions; explicit image model with two cut off parameters ("cut-off1" = 12 Å, "cut-off2" = 14 Å) was utilized. The unit cell was a cube (a = 20 Å). Before simulations, the systems were subjected to steepest descent minimization to relieve unfavorable interactions. After 5 ps of equilibration the systems were simulated for at least 150 ps. Simulations were carried out on room and increasing temperature (300 → 450 K). Higher temperatures were used to overcome the damping force that water exerts and to sample larger conformational space in time available for the simulation.

Acknowledgements

This work was supported by the Ministry of Science and Technology of the Republic of Croatia (grants no. 1-07-179 and 1-08-195) and by the Commission of the European Communities, Brussels (contract no. CI1*-CT91-0891).

References

[1] G. Laćan, V. Magnus, B. Jeričević, L. Kunst, and S. Iskrić, *Plant Physiol.*, 76 (1984) 889–893.
[2] G. Laćan, V. Magnus, Š. Šimaga, S. Iskrić, and P.J. Hall, *Plant Physiol.*, 78 (1985) 447–454.
[3] D.L. Rayle and W.K. Purves, *Plant Physiol.*, 42 (1967) 520–524.
[4] G. Sembdner, D. Gross, H.W. Liebisch, and G. Schneider, in A. Pirson and M.H. Zimmermann (Eds.), *Encyclopedia of Plant Physiology, New Series*, Springer, Berlin, Vol. 9, 1980, pp 281–444.
[5] F.W. Percival, W.K. Purves, and L.E. Vickery, *Plant Physiol.*, 51 (1973) 739–743.
[6] H.M. Brown and W.K. Purves, *J. Biol. Chem.*, 251 (1976) 907–913.

[7] V. Magnus, *Carbohydr. Res.*, 76 (1979) 261–264.
[8] S. Jelaska, V. Magnus, M. Seretin, and G. Laćan, *Physiol. Plant.*, 64 (1985) 237–242.
[9] D. Keglević and M. Pokorny, *Biochem. J.*, 114 (1969) 827–832.
[10] J.B. Szerszen, K. Szczyglowski, and R.S. Bandurski, *Science*, 265 (1994) 1699–1701.
[11] S. Tomić, B.P. van Eijck, J. Kroon, B. Kojić-Prodić, G. Laćan, V. Magnus, H. Duddeck, and M. Hiegemann, *Carbohydr. Res.*, 259 (1994) 175–190.
[12] S. Tomić, B.P. van Eijck, B. Kojić-Prodić, J. Kroon, V. Magnus, B. Nigović, N. Ilić, H. Duddeck, and M. Hiegemann, *Carbohydr. Res.*, 270 (1995) 11–32.
[13] H. Duddeck, M. Hiegemann, M.F. Simeonov, B. Kojić-Prodić, B. Nigović, and V. Magnus, *Z. Naturforsch., Sect. C*, 44 (1989) 543–554.
[14] B. Kojić-Prodić, B. Nigović, D. Horvatić, Ž. Ružić-Toroš, W.L. Duax, J.J. Stezowski, and N. Brescianí-Pahor, *Acta Crystallogr., Sect. B*, 47 (1991) 107–115.
[15] B. Kojić-Prodić, B. Nigović, V. Puntarec, S. Tomić, and V. Magnus, *Acta Crystallogr., Sect. B*, 49 (1993) 367–374.
[16] B. Nigović, B. Kojić-Prodić, and V. Puntarec, *Acta Crystallogr., Sect. C*, 48 (1992) 1079–1082.
[17] B. Nigović, B. Kojić-Prodić, V. Puntarec and J.-D. Schagen, *Acta Crystallogr., Sect. B*, 48 (1992) 297–302.
[18] S. Tsurumi and S. Wada, *Plant Cell Physiol.*, 27 (1986) 559–562.
[19] R. Plüss, T. Jenny, and H. Meier, *Physiol. Plant.*, 75 (1989) 89–96.
[20] A. Östin, A.M. Monteiro, A. Crozier, E. Jensen, and G. Sandberg, *Plant Physiol.*, 100 (1992) 63–68.
[21] D.M. Reinecke and R.S. Bandurski, *Plant Physiol.*, 71 (1983) 211–213.
[22] V. Magnus, D. Vikić-Topić, S. Iskrić, and S. Kveder, *Carbohydr. Res.*, 114 (1983) 209–224.
[23] C.K. Johnson, ORTEPII, Report ORNL-5138, Oak Ridge National Laboratory, TN, USA, 1976.
[24] G.A. Jeffrey, *Acta Crystallogr., Sect. B*, 46 (1990) 89–103.
[25] B. Kojić-Prodić, B. Nigović, S. Tomić, N. Ilić, V. Magnus, Z. Giba, R. Konjević, and W.L. Duax, *Acta Crystallogr., Sect B*, 47 (1991) 1010–1019.
[26] G.A. Jeffrey and J.H. Yates, *Carbohydr. Res.*, 74 (1979) 319–322.
[27] D. Cremer and J.A. Pople, *J. Am. Chem. Soc.*, 97 (1975) 1354–1358.
[28] J.F. Stoddart, *Stereochemistry of Carbohydrates*, Wiley-Interscience, New York, 1971.
[29] Cambridge Structural Database System, version 5.08, Cambridge Crystallographic Data Centre, Cambridge, October 1994.
[30] T. Srikrishnan and S.H. An, *J. Carbohydr. Chem.*, 7 (1988) 571–581.
[31] J.P. Bouquiere, J.L. Finney, M.S. Lehman, P.F. Lindley, and H.F. Savage, *Acta Crystallogr., Sect. B*, 49 (1993) 79–89.
[32] Th. Steiner and W. Saenger, *Acta Crystallogr., Sect D*, 49 (1993) 592–593.
[33] Th. Steiner, *J. Chem. Soc., Chem. Commun.*, 49 (1994) 2341–2342.
[34] Th. Steiner, *Acta Crystallogr., Sect D*, 49 (1995) 93–97.
[35] W. Klyne and V. Prelog, *Experientia*, 16 (1960) 521–523.
[36] P. Dauber-Osguthorpe, V.A. Roberts, D.J. Osguthorpe, J. Wolff, M. Genest, and A.T. Hagler, *Proteins: Structure, Function and Genetics*, 4 (1988) 31–47.
[37] J.R. Maple, T.S. Thacher, U. Dinur, and A.T. Hagler, *Chem. Design. Autom. News*, 5(9) (1990) 5–10.
[38] S.W. Homans, *Biochemistry*, 29 (1990) 9110–9118.
[39] E. Fischer and E.F. Armstrong, *Ber. Dtsch. Chem. Ges.*, 35 (1902) 833–843.
[40] E. Erwig and W. Koenigs, *Ber. Dtsch. Chem. Ges.*, 22 (1889) 2207–2213.
[41] L.J. Haynes and F.H. Newth, *Adv. Carbohydr. Chem.*, 10 (1955) 207–256.
[42] G.M. Sheldrick, in G.M. Sheldrick, C. Krueger, and R. Goodard (Eds.), *Crystallographic Computing 3*, Oxford University Press, 1985.
[43] G.M. Sheldrick, SHELX77, Program for Structure Determination, University of Cambridge, 1983.
[44] A.L. Spek, in D. Sayre (Ed.), *Computational Crystallography*, Clarendon Press, Oxford, 1982, p 528.
[45] BIOSYM (1994) DISCOVER, version 2.96, Biosym Technologies, 10065 Barnes Canyon Rd., San Diego, CA 92121, USA, 1994.
[46] S.W. Homans and M. Forster, *Glycobiology*, 2 (1992) 143–151.
[47] M.J. Forster and B. Mulloy, *Biopolymers*, 33 (1993) 575–588.
[48] P.K. Warme and H.A. Scheraga, *Biochemistry*, 13 (1974) 757–767.